ADVANCED MATERIALS INTERFACES
www.advmatinterfaces.de

Liquid Metal Switches for Environmentally Responsive Electronics

*Raymond Adam Bilodeau, Dmitry Y. Zemlyanov, and Rebecca K. Kramer**

More than six decades ago, liquid mercury was used to demonstrate the potential of room-temperature liquid metals as soft circuit elements.[1] This sparked an exploration into using liquid metals to conduct both heat and electricity in systems that are either physically compliant or reconfigurable. General use of mercury is impeded by its toxicity, so in the past decade gallium-based room-temperature liquid metals have begun to replace mercury for use in conductive circuitry applications. The value of flexible and adaptable liquid metal conductors is probably best exemplified in recent soft robotics design, development, and control applications.[2–5] In order to harness the full potential of liquid metal circuitry, more investigation is necessary into the fundamental principles governing liquid metals' behavior, as well as possible applications for these liquid metals.

Gallium-based alloys can be found in a liquid form at both room and elevated temperatures. At high temperatures (>600 °C), researchers have controlled the motion of liquid gallium arsenide via chemical decomposition of the alloy, controlling the direction of motion via surface crystallinity of the substrate.[6–9] Other high-temperature gallium alloys have been controlled and directed by surface roughness.[10] This previous work demonstrates the feasibility of metallic droplet manipulation, but the high temperatures involved make it impractical for common, everyday use.

Gallium-indium-based room-temperature liquid metal alloys (usually eGaIn, a eutectic gallium-indium alloy, or galinstan, a gallium-indium-tin alloy) have become even more commonplace as researchers develop reconfigurable and soft electronic devices. These gallium alloys have appeared in a number of soft electronics[11] including self-healing electronics,[12] tunable electronics,[13] and stretchable sensors.[14] In these examples, the liquid metal is manipulated through encapsulation inside of a flexible polymer, enabling mechanical shape-giving and shape-changing of soft electronics.

There is also a growing interest in the ability to manipulate the geometry and electric path of the liquid metal via non-mechanical techniques. By powder coating small droplets, researchers created microscopic marbles,[15,16] which Tang et al. moved by shining a light on the powder-coated surface.[17] High-frequency magnetic fields can drive galinstan droplet motion,[18] providing a second system for non-mechanical liquid metal manipulation. Zhang et al. fed aluminum chips to a galinstan droplet as fuel for self-propulsion,[19] and have since developed non-contacting magnetic controls for the droplet.[20] Finally, a large category of recent research has used electricity to create relative motion and shape change in liquid metals,[21–23] enabling non-contacting pumps for microfluidic flow[24] and cooling,[25] self-destructive circuitry (path-destructive liquid metal droplet motion),[26] and most recently as a source for rigid-body locomotion.[27]

It is well known that gallium oxidizes rapidly in normal atmospheric conditions, or in any environment with oxygen levels above 1 ppm,[11,28,29] forming a gallium oxide that has been studied in detail.[30–32] This oxide is solid at room temperature and forms a nanoscale stabilizing shell around liquid gallium indium alloys, enabling the liquid metal to be patterned onto, and subsequently adhere to, many different material surfaces (via a plethora of techniques).[33] If the oxide is removed, the liquid metal loses its adhesion to the substrate and will reflow under the influence of gravity (or other forces), enabling a fixed liquid metal pattern to change. In other words, oxide removal enables real-time, non-mechanical manipulation of liquid metals. This has typically been done either in nitrogen boxes (via passive oxide prevention) or in chemical etchant baths (via active oxide removal).[18,19,21,24–26] Unfortunately, these methods require enclosed (air-tight or water-proof) chambers that limit the practical applications for manipulation of liquid metal circuits on the fly, as the circuits must remain inside the chamber.

The two main etchants used for aqueous oxide removal are hydrochloric acid (HCl, a low-pH acid)[15,18,21,30,31,34] and sodium hydroxide (NaOH, a high-pH base).[19,21,22,24–26] Both of these etchants mix readily with water and can be contained safely at high concentrations. A non-aqueous alternative for oxide removal comes through exposing the liquid metals to concentrated HCl vapor,[35–39] but practical applications of this are generally limited to environments that can withstand the presence of a highly corrosive gas.

In this work, we demonstrate control over the surface oxide of liquid metal droplets, which in turn controls the wetting and adhesion of those drops on a substrate, using purely environmental stimuli. We compare the use of highly acidic HCl and highly alkaline NaOH (in solution) in removing the oxide to release pinned droplets. We show that although both solvent solutions result in high contact angles between the droplet and the substrate, NaOH achieves this result at a rate that is orders of magnitude faster than HCl. We further explore the use of neutral distilled water to regrow the oxide and manipulate the contact area of the liquid metal droplet on the surface, causing the droplet to readhere to the substrate. Finally, we apply this environmentally controlled depinning and repinning

R. A. Bilodeau, Prof. R. K. Kramer
Department of Mechanical Engineering
Purdue University
West Lafayette, IN 47907, USA
E-mail: rebeccakramer@purdue.edu
Dr. D. Y. Zemlyanov
Birck Nanotechnology Center
Purdue University
West Lafayette, IN 47907, USA

DOI: 10.1002/admi.201600913

Table 1. Contact angles of galinstan droplets on various substrates, immersed in either 1 M HCl or 1 M NaOH. ± value is one standard deviation.

Etchant	Substrate	Contact angle [°]
HCl (1 M)	Glass	164 ± 1.6
	Silicon	161 ± 1.3
	PDMS	159 ± 4.6
NaOH (1 M)	Glass	165 ± 0.8
	Silicon	162 ± 0.5
	PDMS	164 ± 2.1

technique, demonstrating its viability for creating both reconfigurable electronics and fully reversible liquid metal switches. The methods presented herein enable the use of simpler aqueous techniques for liquid metal manipulation, while subsequently permitting the final liquid metal morphology to be removed from the aqueous medium.

Oxide Removal Rate Measured by Contact Angle: Since both HCl and NaOH have been used to remove the gallium oxide layer surrounding liquid metal droplets, we begin by comparing the influence of the two chemical etchants. We measured the contact angle of galinstan droplets on the surface of various substrates while submerged in both HCl and NaOH solutions at room temperature (see the Experimental Section for details). Our results are presented in **Table 1**. All equilibrium contact angles were roughly the same (≈160°) in 1 M HCL and NaOH, which is lower than previously reported values.[30] For glass and silicon substrates, data variance was low; but with a silicone elastomer as the substrate (polydimethylsiloxane; PDMS), the droplets had a noticeable variation in their final contact angles (with one droplet never getting higher than 153°). We suspect that this is due to chemical interaction between the etchant and the PDMS, combined with batch variations inherent to PDMS.[40] We also note that droplet buoyancy plays a role in contact angle when measured in aqueous solutions. Therefore, the contact angles measured are higher than reported contact angles of liquid metal droplets with the oxide removed via HCl vapor treatment.[36]

Comparing time stamps for each profile photograph, we approximated the time-scale required to develop the maximum equilibrium contact angle for each droplet. At the same concentrations (1 M), HCl took much longer than NaOH to develop the maximum contact angle, even though the treatment method was the same. The time difference was largest on a PDMS substrate (see **Figure 1**), likely due to the softer and more porous nature of the substrate. When placed in an HCl bath on PDMS, galinstan droplets consistently took several hours to develop their maximum contact angle (like the droplet shown in HCl in Figure 1). When placed in NaOH, the droplets would achieve a maximum contact angle in a very short amount of time (on the order of minutes).

In the context of reconfigurable electronics, this has immediate ramifications on the configuration rate. The choice of chemical etchant seems to have a large degree of influence on the speed at which an adhered droplet can be released from a substrate. Since oxide removal is the key to releasing a droplet,

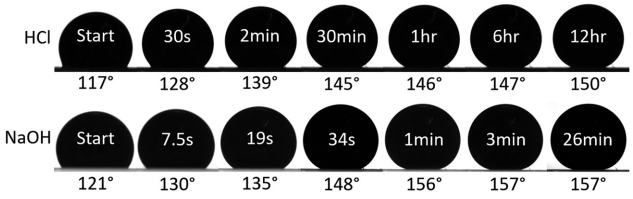

Figure 1. The evolution of the contact angle and droplet profile for a galinstan droplet placed on a flat PDMS in either a 1 M HCL or a 1 M NaOH bath. It should be noted that the last frame of the NaOH shows the droplet completely depinned (it has begun rolling).

we further investigated the speed at which the surface oxide is removed by HCl and NaOH from a liquid metal droplet.

Oxide Removal Rate Measured Optically: To the authors' knowledge, there have been no studies on the chemical kinetics of gallium oxide reacting with HCl and NaOH. To measure the time it takes to remove the oxide by chemical etchants, we developed a simple reflectance experiment, as shown in **Figure 2**. We coated small, chemically inert platforms with PDMS (for adhesion) and then, using a syringe, we placed very large galinstan droplets (diameter ≈ 8 mm) onto the PDMS. The droplets sat for 24 h to encourage oxide adhesion. We then removed the liquid metal from inside of the droplet with a syringe, leaving the encapsulating oxide behind. As the surface area of the droplet decreased from its original spherical area to an area approximately the size of the droplet's circular profile,

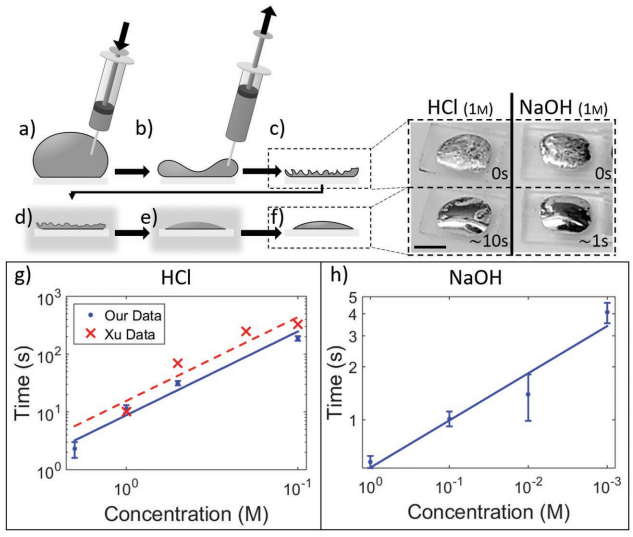

Figure 2. Experimental method for comparing galinstan oxide removal rates by HCl and NaOH. a) Large droplets of galinstan are placed on a PDMS substrate, and allowed to sit for 24 h. b) The liquid metal inside of the droplet is then removed, c) causing the solid oxide layer to develop a visible texture. d) When the textured oxide is immersed into a chemical etchant bath, e,f) the exterior of the oxide begins to dissolve until the original, reflective surface is restored. The time it takes to move from (d) to (e) depends on the chemical etchant used, and the insets for (c) and (f) show examples of textured droplets treated by either HCl or NaOH, along with the time required to remove the visible oxide. g,h) We tested the removal rate of the oxide at several concentrations, and present the data in logarithmically scaled plots. The data gathered by Xu et al. using rheometry (in HCl)[30] is presented alongside ours, as validation of our method. Scale bar is 4 mm.

the solid oxide skin buckled and wrinkled, developing a dull gray hue. The buckled oxide scatters light instead of reflecting it as a fresh oxide layer or the pure liquid metal does. Once the droplets are submerged in either NaOH or HCl baths, the buckled oxide is chemically removed and a reflective surface is restored to the droplet. Filming the process allowed us to record the time it takes to change the droplets surface. This optical test confirmed the difference between the speed at which HCl and NaOH remove the gallium oxide layer as observed when studying contact angles.

We set up all of the droplets onto platforms simultaneously, and randomly selected droplets for submersion in either a 1 M HCl or 1 M NaOH solution. Each bath was prepared fresh and used only once, and the droplets were submerged with chemically inert tweezers to prevent any interaction of the tweezers with the acid/base. Examples of the droplets are displayed in Figure 2, and a video of the tests is available in the Supporting Information. The droplets submerged in HCl took between 9 and 13 s for their oxide layers to be removed (average 11.35 s ± 1.7 s standard deviation). The galinstan droplets immersed in NaOH, however, had their oxide skins removed in 0.58 s (average) with a 0.045 s deviation—most of the deviation and error being caused by the frame rate of the camera used to film the submersion instead of the actual chemical reaction.

This test provides further evidence for a comparative advantage of using NaOH over HCl in removing the gallium oxide layer from gallium-based room-temperature liquid metals. With the initial success of comparing the 1 M concentrations using this technique, we then expanded our tests to include various concentrations of HCl and NaOH. Since 1 M NaOH was already very fast at processing, we proceeded to test 0.1, 0.01, and 0.001 M. Since 1 M HCl was already acting slowly, we performed the test on a range of molarities between 2 M (to speed the process up) and 0.1 M.

The final results of our optical tests are displayed in the log-log graphs of Figure 2. Each data point is an average and the error bars represent a 95% confidence interval on the mean time. We fit a simple power-law curve to the data ($y = bx^m$), where the constant b represents the speed of oxide removal at 1 M concentration and the constant m correlates the change of the etchant concentration and the time required to remove the oxide. The HCl fitted parameter m is −1.417, indicating a large change in oxide removal time for small changes in concentration. For NaOH this parameter was found to be −0.268, an order of magnitude smaller than the HCl, indicating minimal change in oxide removal times at even very low concentrations. Although the trend lines do not contact all of the confidence intervals, it is important to note that the plotted confidence intervals are representative of deviation in the measured time only and do not take into account any uncertainty in the molarity of the chemical etchant baths.

To validate our procedure, we compared our data to the work performed by Xu et al.[30] who used parallel-plate rheometry to characterize the influence of various concentrations of HCl on gallium oxide. By actively removing the oxide with HCl during the parallel-plate test, they were able to observe a change in the mechanical properties of the oxide over time, until they observed complete mechanical breakdown, suggesting oxide removal. Their results do not have the timescale resolution as our simple setup does, but we interpreted their data to develop an oxide removal time versus concentration curve, and plotted their data against ours. Via curve-fitting the b and m constants of the power-law equation, we found that their data set and our HCl-treated data set had nearly identical slopes (ours with $m = -1.417$ compared to theirs of $m = -1.501$), with an offset on the b value likely because their setup provided greater information about the complete oxide removal.

Combining this quantitative test with the qualitative work shown in Figure 1, we can conclude that, at the same concentration, NaOH will release a droplet of pinned galinstan much more rapidly than HCl will by dissolving away the gallium oxide faster. It is not until the concentration of HCl is increased to 2 M that the oxide is removed at a rate similar to very low concentration NaOH (0.005 M).

Oxide Removal Rate Measured by Surface Tension: Surface tension is a key part of both liquid–substrate adhesion (in the contact angles developed by a liquid) and droplet mobility. To compare galinstan droplets' surface tension in either HCl or NaOH baths, we performed simple goniometry measurements, and our results can be found in **Table 2**. We started by measuring the surface tension of galinstan droplets suspended in oxygen-rich air. The surface tension we measured was 593 ± 46 mN m^{-1} (95% confidence), exhibiting a large variation, but always greater than 500 mN m^{-1}, as expected.[11]

Unlike in our contact angle tests, we were not able to have both the HCl and the NaOH at 1 M concentrations. When we extruded a galinstan droplet into a 1 M NaOH solution, the chemical reaction between the galinstan and the etchant was so vigorous that the droplet would disconnect from the extrusion needle before we could begin measurements. Decreasing the concentration to 0.1 M enabled rapid oxide removal and droplet stabilization, while permitting measurements to be made. This required change in concentration for our goniometry tests provides a third demonstrable difference between HCl and NaOH in chemically treating galinstan.

The final surface tension of galinstan in both the HCl and NaOH baths was 470 ± 12 and 486 ± 6 mN m^{-1} (95% confidence), respectively. Though the averages are slightly different, the confidence intervals overlap sufficiently to negate any distinction between the two. We attribute the uncertainties of the values in Table 2 to the highly spherical nature of the droplets and therefore low bond numbers[41] (≈0.1). Although bond numbers <1 are desired when using drop shape analysis to determine surface tension,[42] extremely low bond numbers (<0.1) cause errors in the fitting parameters when digital systems are in use.[43] Our droplets were close to this range, causing a slightly larger variance in the measured values than

Table 2. Surface tension on galinstan droplets in various environments. ± value is 95% confidence on mean.

Environment	Surface tension [mN m^{-1}]	Time to equilibrium
Air	593 ± 46	85 min
HCl (1 M)	470 ± 12	1.5 h
NaOH (0.1 M)	486 ± 6	0 s
H_2O	230–350	6 h

we would have desired. Regardless, we conclude that the surface tension measured in both etchants is close enough to be equivalent.

Oxide Regrowth and Transformation Measured by Surface Tension: Since a 1 M solution of either HCl or NaOH has a significant water component, we wanted to determine the influence of clean water on the surface tension of liquid metals. This would help us determine if the chemistry of water was having a significant impact on the surface tension of the liquid metal droplets, or if the dissolved acid (or base) was driving the measured surface tension values. Following the same experimental procedure we used for HCl and NaOH, we measured the surface tension of galinstan droplets in both distilled and deionized water. In both types of water, the droplets registered an initial surface tension profile at well over 500 mN m^{-1}, but over the period of hours it would drop between 40% and 60%, sinking to a range anywhere from 350 to 230 mN m^{-1} (see Table 2). This surface tension range is nearly half the value of the other mediums.

In goniometry, the time to achieve equilibrium surface tension depends primarily on the chemistry between the droplet and the surrounding environment.[43] Droplets extruded into 1 M HCl took around 1.5 h to come to an equilibrium whereas droplets extruded in the 0.1 M NaOH bath achieved an equilibrium surface tension nearly instantaneously. In water, however, the droplets often took over 6 h to come to an equilibrium state. The extreme drop in surface tension over such a long time can only be attributed to a slow chemical change of the surface properties of liquid metal by the surrounding water. This finding is supported by the work of Khan et al. who performed X-ray photoelectron spectroscopy (XPS) studies on the oxide layer and noted the generation of a gallium hydroxide alongside the normal gallium oxide when the droplet had been exposed to water.[44] Using rheometry, they demonstrated that the hydroxide layer has a much lower modulus of elasticity than gallium oxide. This helps us to understand the results of our goniometry. When we initially extruded a droplet of liquid metal into water, the liquid metal likely used the dissolved oxygen in the water to create the characteristic thin gallium oxide layer. Over time, however, the water reacted with the surface of the droplet, changing the surface into the softer hydroxide. Since the stiff, stabilizing oxide had been chemically changed to a weak hydroxide, the droplet distends under its own weight (see Figure S1, Supporting Information). This explains both the long time required to develop the final equilibrium surface tension and the large change in surface tension. The long time was because of the slow chemical kinetics of the water reacting with the gallium oxide (having to diffuse through the whole layer of gallium oxide), and the large change in surface tension is due to the newly formed, weaker, hydroxide exterior.

Previous studies into the effects of water on eGaIn–surface interactions have mostly focused on the short-term effects of a thin "slip-layer" of water.[23,44] Khan et al. observed that oxidized eGaIn could slide across a surface that it would normally stick to, when there is a layer of water present.[44] They also showed that as the substrate dries, the oxide sticks to it again. During our experiments, we observed similar slipping of liquid metal droplets, but only on short time scales. Given longer time scales, we observed that a droplet of gallium-based liquid metal will adhere to a surface, regardless of the presence of water.

Oxide Regrowth and Transformation Measured by XPS Analysis: We performed an XPS analysis to characterize the chemical effect of various surface treatments on galinstan. We tested four different conditions: droplet submersion in HCl followed by a quick rinse in water or a 24 h immersion in water, and droplet submersion in NaOH followed by a quick rinse in water or a 24 h immersion in water. Rinsed droplets were dipped in a clean bath for 2 s, and afterward were immediately dried. Soaked droplets were immersed for 24 h to compare the XPS results to the rinsed droplets and determine which surface properties were caused by the chemical etchant and which results stem from the water baths. A list of all the spectra analyzed for these results is contained in the Experimental Section.

Figure 3 shows the XPS results of the four different conditions over the In 4d/Ga 3d/Sn 4d region. With the rinsed droplets, we anticipated observing an effect similar to that reported by Kim et al.,[36] who demonstrated that eGaIn droplets treated with HCl vapor grow a gallium chloride and indium chloride shell in place of the gallium oxide. However, we did not find any trace of these chloride shells. Instead, it appeared that almost all of the influences of either chemical etchant (HCl or NaOH) were completely removed when the droplets were rinsed in H_2O, making the XPS results nearly identical. We suspect that any alternative shells grown around the galinstan droplets by either the NaOH or the HCl were completely removed during the rinsing process. Notably, the surface concentration

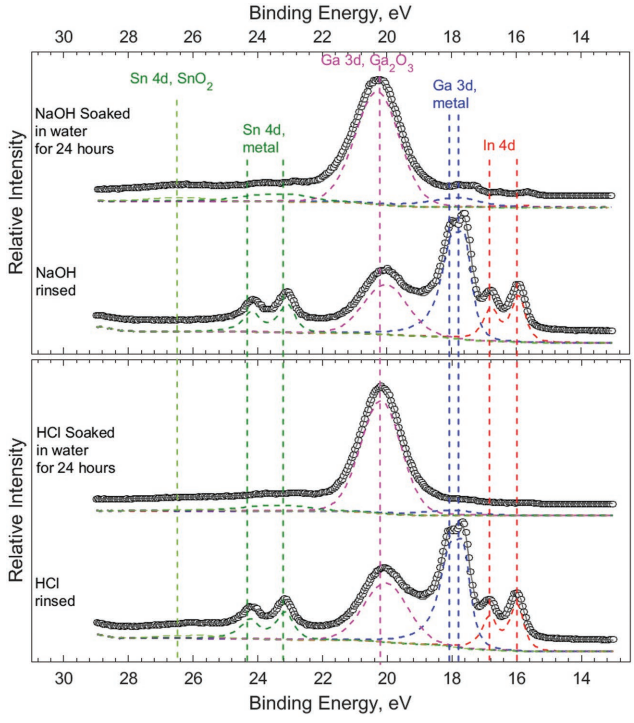

Figure 3. In 4d/Ga 3d/Sn 4d XPS spectra obtained from the samples that were treated with NaOH (top panel) and HCL (bottom panel). Spectra in each panel obtained following soaking for 24 h (top spectrum) and a short rinse (bottom spectrum).

of gallium was slightly enriched after the rinsing (85 at% vs 78 at% for ideal galinstan), and there was a significant amount of oxygen present in the spectrum (not shown in the figure). Using the ratio between the metal and oxide components in Ga 2p (not shown) and 3d, we calculated the thickness of the regrown gallium oxide at about 3 nm. The details of such calculations can be found elsewhere.[45–48]

As seen in Figure 3, both rinsed samples showed the Sn 4d (metal) peaks, but the soaking treatment resulted in disappearance of tin from the surface of the droplet: the Sn 4d (metal) peaks are barely visible. Indium concentration follows the same trend: the amount of indium visible from the surface greatly decreased following soaking in H_2O. Inversely, there was an increase of covalently bonded gallium (shown as a shift of the Ga 2p and 3d peaks from the pure-metal energy level), indicating more oxide had grown on the surface. From these data, we estimated a new oxidized gallium layer thickness at 7 nm. This doubling of the exterior shells' thickness explains the disappearance of the tin and indium, as they were no longer visible from the surface of the droplet. Though the chemical composition of gallium oxide is mainly Ga_2O_3,[11] the soaked sample showed much higher amount of OH groups as evidenced from the O 1s spectra (not shown), confirming a chemical shift toward gallium hydroxide on the surface of the droplet, as expected.[44,49,50]

From our XPS results, it is clear that gallium oxide thickness correlates with water treatment: rinsing resulted in 40%–44% of gallium on the surface in the form of oxide, whereas soaking resulted in 90%–93%. Furthermore, these results show evidence that the droplet's oxide layers, which had been chemically removed by the HCl or NaOH, were completely restored by simply rinsing the droplets in water. This happened for both the HCl and NaOH treated droplets, so we can easily conclude that the original method of chemically treating the galinstan is unimportant when oxide restoration is performed by rinsing with water. Finally, there is a time element involved in exposing liquid metals to water: further exposure to water (beyond rinsing) results in the oxide layer growing in thickness while changing partially into a hydroxide layer.

Oxide Regrowth and Transformation Measured by Contact Area: Since water removes the surface effects of HCl and NaOH, we could use it as a method to reattach droplets that had been removed via the chemical etchants. We tested this on a droplet through a simple experiment: we soaked a galinstan droplet in NaOH to remove its oxide, and then placed it onto a glass substrate immersed in distilled water. We tracked the profile of the droplet over a 4 h period, and recorded the radius of the droplet's contact area on the substrate. From this information, we calculated the contact area as it changed with time and present our findings in **Figure 4**. Although the droplet began to adhere on the order of minutes, the increasing contact area improved the adhesion over the period of the test.

The contact angle did not change much during the test, but the contact area of the droplet increased significantly with increasing time submerged in H_2O. As is visible in the inset images in Figure 4, the original circular droplet shape collapsed down into a flattened ellipsoid, maintaining a high contact angle as the droplet spread outward and enabling a large contact area on the substrate.

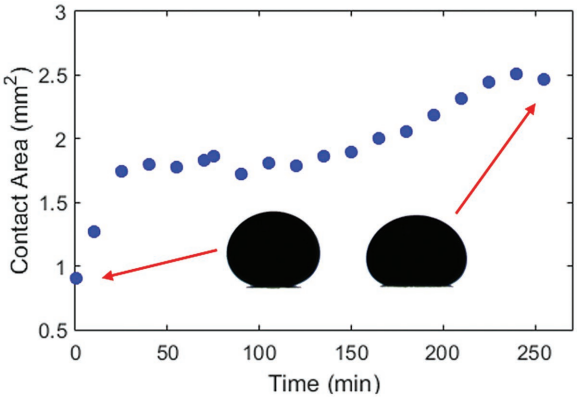

Figure 4. Changing contact area between a galinstan droplet and a glass substrate in water. The droplet was initially removed from the substrate using a 1 M NaOH solution. The NaOH was replaced with clean water, and the droplet collapse was observed for 4 h. The inset shows the droplet's initial and final states in the water.

As with the surface tension work reported previously, we hypothesize that the changing contact area (and adhesion to the substrate) is due to the rapid triple effect during the initial submersion of the droplet. First, the water removed any influence of the NaOH. Second, the dissolved oxygen grew a gallium oxide shell. Third, the water quickly changed the outer surface of the shell to a hydroxide, leaving the rest of the oxide untouched. While continuing to soak in the bath, the hydroxide slowly diffused through the whole thickness of the shell, weakening the droplet walls and causing the spherical droplet to collapse under its own weight. This process resulted in a pulsing/shape changing effect on the droplet, as evidenced from Figure 4 between 50 and 150 min, and can be seen in Video S2 (Supporting Information) between timestamps 0:50 and 1:00.

We note that after the water was removed, the droplet had fully adhered to the substrate. We tested other techniques (details in the Supporting Information) to repin the droplet, but they were not as successful as this method.

Liquid Metal Droplet Mobility: With droplet adhesion driven by the gallium oxide layer on the liquid metal, we can free the droplet by removing the oxide layer with either HCl or NaOH, causing the droplet to roll freely on the substrate. Afterward, we can repin the droplet to the substrate by rinsing it with water, encouraging regrowth of either a gallium oxide or a gallium hydroxide layer on the surface of the droplet. These two chemical tools are all that is required to remove galinstan droplets from a substrate and then fix them in a desired location, and we now demonstrate the potential for this to be applied in manipulating liquid-metal-based electronics.

Figure 5 shows our results being applied for environmentally stimulated liquid metal droplet mobility. We depinned a droplet from one location, enabling it to roll to a new location, and then pinned the drop back to the substrate. Figure 5a shows the droplet of galinstan that has been adhered to a substrate in an initial position. The droplet is then exposed to a 1 M NaOH bath (Figure 5b), which causes the droplet to depin from the substrate and change location (Figure 5c) by gravitational forces. Finally, by replacing the NaOH bath with water, the droplet is

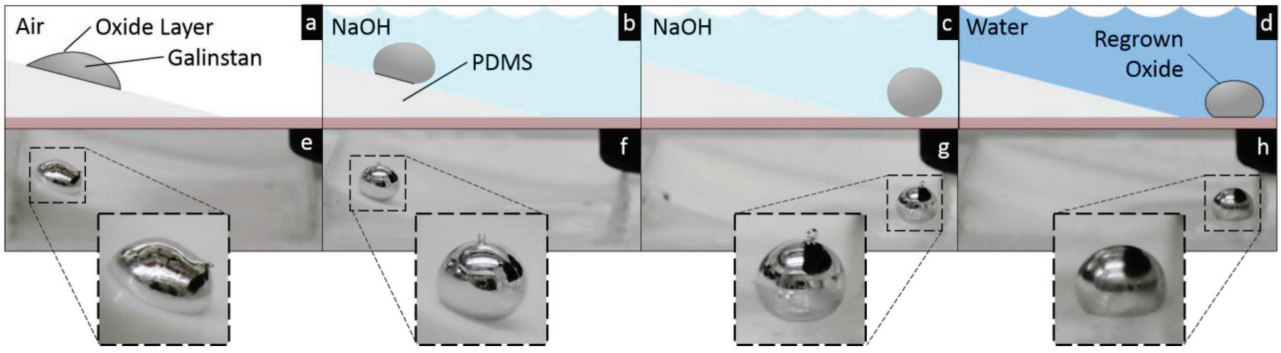

Figure 5. Controlling the location and fixity of a liquid metal droplet. a) The droplet is pinned to the substrate in air. b) Submerging the droplet in 1 M NaOH causes the droplet to depin. c) The depinned droplet moves under gravitational force. d) The droplet is repinned to the substrate through an H_2O bath. e–h) Photographs of the active test, matching the diagrams in (a)–(d). Inset boxes are ≈3 mm × 3 mm.

able to re-attach to the substrate in the final position (Figure 5d). The high contact angle on the droplet enables extremely rapid droplet motion once the droplet has been depinned. Furthermore, this droplet mobility is controlled by the environment alone, with gravity being the only source of force. We see future opportunities to combine this process with environmentally controllable surface morphology, which would in turn enable control over droplet locomotion direction, as well as applications in connecting/disconnecting circuitry for reconfigurable logic.

Liquid Metal Switch: Using environmental stimuli, we also demonstrate the ability to repeatedly disconnect and reconnect a conductive pathway, as shown in **Figure 6**. We connected an LED and a droplet of galinstan in series in a circuit (visible in Figure 6e). The galinstan droplet was in a special environmental chamber with two conductive tungsten leads emerging from the chamber walls for the droplet to rest on. We alternately tested the resistance across the galinstan droplet and applied a power source to the whole circuit (Korad KA3005D DC power supply, set to provide either a max of 3.3 V or 10 mA) to see if the LED would illuminate. For each test, we cycled the fluid in the environmental chamber, starting with air and then filling the chamber with a 1 M NaOH bath, continuing on to distilled water, and then drying all the water out of the chamber with air again. Figure 6a–d is a schematic representation of the cycle, showing a profile view of the droplet and how it contacts the electrodes based on the chemical bath in the chamber. A video of the droplet profile during a cycle is available in the Supporting Information.

We were able to disconnect and reconnect the LED using the NaOH bath to lift the droplet up, disconnecting the electrodes,

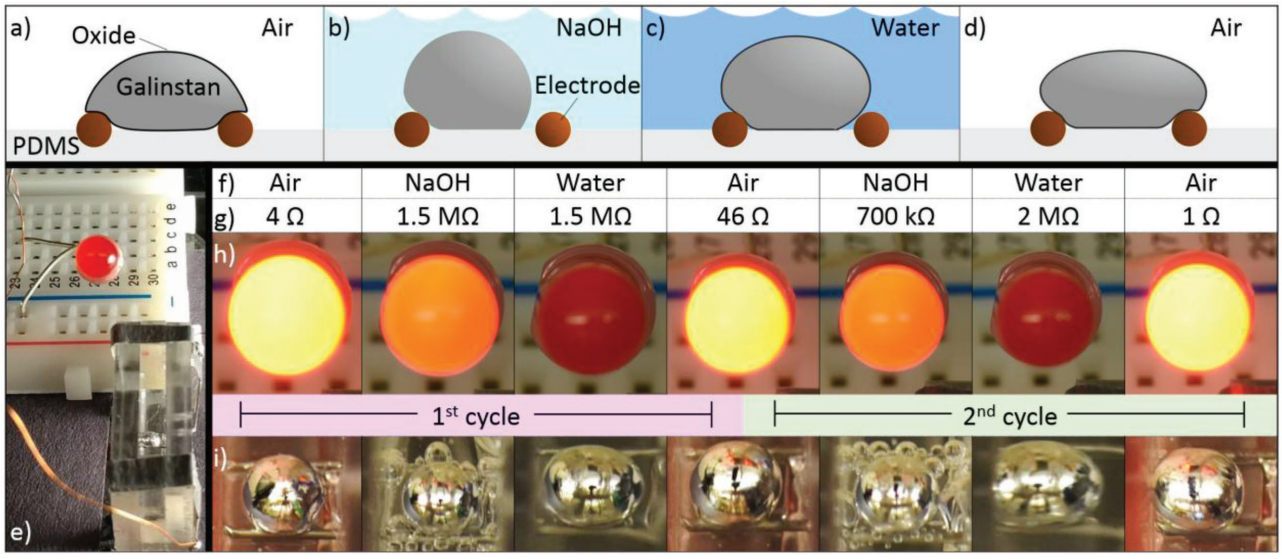

Figure 6. Opening and closing a circuit via chemical manipulation of a liquid metal droplet. a–d) Schematic representation of the side profile of the droplet during one air-NaOH-water-air treatment cycle: a) initial state, b) submersion in 1 M NaOH disconnecting the circuit, c) replacing the NaOH with water encourages the droplet to collapse, and d) the droplet is dried reconnecting the circuit. e) A photograph of the environmental chamber and LED used for this test (for scale, the LED is 3 mm dia). h) A series of photographs of the LED with power supplied to the circuit during two consecutive cycles. i) Close-up views of the droplets in the chamber when power was supplied, along with f) the chamber environment and g) a measurement of the resistance across the chamber's leads, during the two consecutive cycles. A video of the droplet profile during a third cycle is available in the Supporting Information.

and the water bath to collapse the droplet back down, reconnecting the electrodes. Figure 6f,g describes the current stage of the cycle and the resistance measured across the liquid metal droplet, while Figure 6h,i is a series of simultaneous photographs of the LED and the galinstan droplet during each stage of the cycle. It is important to note that although the NaOH bath disconnected the liquid metal droplet from the circuit, the NaOH itself was able to conduct electricity via electrochemical means. This is why although the resistance is very high with both the NaOH and the water baths, the LED illuminates (partially) when power is applied during the NaOH portion of the cycle. Furthermore, the electrochemical interaction is what causes the gas bubbles visible around the galinstan droplet in Figure 6i during this portion of the cycle (also visible in the video). Once we rinsed the NaOH away with distilled water, the water no longer connected the electrodes and the LED ceased to illuminate. We also note that, although not shown in the figure, if we rinse out the NaOH from the chamber and then rapidly dry the water from the chamber (with a small fan) the droplet holds its new shape, keeping the circuit open. The circuit can then be closed at any time by soaking the droplet in water.

Having successfully developed a system where we were able to completely disconnect and reconnect the circuit via environmental stimulation, we cycled the circuit to ensure repeatability. In Figure 6 we show two consecutive disconnect and reconnect cycles, without changing the liquid metal droplet or any other part of the circuit. We cycled it a third time, while recording the video found in the Supporting Information. In the video, we demonstrate the mobility of the chamber after the droplet had dried, proving that liquid metals can be manipulated, reconfigured, and then pinned in place so that circuits built from these liquid metals can be removed from environmental control chambers.

In this paper, we have quantified the influence of acidic (HCl), alkaline (NaOH), and neutral (water) aqueous environments on liquid metal droplets prone to surface oxidation. Our results demonstrate the use of environmental stimuli to control the removal, formation, and transformation of surface oxide on liquid metal droplets, thereby controlling the adhesion of the droplets on various surfaces. While previous studies have shown liquid metal oxide removal in HCl and NaOH baths, our results indicate the timescales for these removals differ by orders of magnitude at similar concentrations, with NaOH emerging as the more aggressive etchant. Furthermore, we have shown that rinsing the liquid metal droplet in water reverses the effects of HCl and NaOH, allowing formation of a surface oxide at short timescales and surface hydroxide at long timescales, which differ in mechanical properties but both encourage liquid metal adhesion to the substrate. Finally, we have employed our findings to demonstrate liquid metal droplet mobility on-demand and environmentally responsive liquid metal switches.

Experimental Section

The three types of substrates primarily used were P-type silicon (Wafer World), microscope slide glass (Home Science Tools), and Sylgard 184 as PDMS (Dow Corning). These substrates were used as they are representative of substrates typically utilized for liquid metal patterning since galinstan readily adheres to them. Galinstan (68.5% Ga, 21.5% In, 10% Sn by weight) was obtained from Sigma Aldrich, and used as-received from the manufacturer. HCl (Fisher Chemical) and NaOH (Macron Fine Chemicals) were obtained in either concentrated or dried forms and mixed with water to get the desired concentrations.

Contact Angles: To measure contact angles, galinstan droplets were set on a cleaned substrate for 3–5 min, covered. This setting time allowed the droplets to adhere to the surface, so that the droplet could be placed in the bath without dislodging it. The substrates and droplets were then placed in a bath of either NaOH (1 M) or HCl (1 M). Photographs of the droplet profile were taken regularly while the etchant slowly lifted the edges of the droplet and the contact angle maximized. At least three different droplets of different sizes were profiled and the results returned were an average of the different droplets. HCl and NaOH were used in both 1 molar concentrations for the bath, and each was tested on the following substrate types: glass, silicon, and PDMS. To ensure that the PDMS substrate was flat, uncured PDMS was spin-coated onto small glass slides (SCS G3-8 Spin Coater) at 2000 rpm for 2 min, before curing them at 60 °C for 2 h. Each substrate was used only once for a single galinstan droplet, to prevent any acid/base etching of the surface from effecting subsequent results. All tests were performed at room temperature (≈25 °C).

Goniometry: Pendent drop shapes were recorded and measured in a goniometer (Ramé-Hart Instrument Co.) capable of performing oscillating pendent drop measurements (though this feature was not enabled). Each test was performed in a similar manner, using a non-air gap technique in which the water inside of the pipette tip directly contacts the liquid metal. This removed any viscoelastic effects of a compressible air pocket while extruding the liquid metal droplets. 5–8 mL droplets of liquid metal were extruded directly into the medium being used for the analysis (air, water, HCl, or NaOH) and briefly allowed to stabilize for up to 30 s, to enable vibrations from the extrusion process to die off. At this point, the surface tension and volume of the droplet were recorded at intervals between 10 and 30 s (depending on the total length of the test) to allow the droplet to achieve equilibrium surface tension. The surface tension was then recorded as an average of the equilibrium tail of the data. Initial droplet volumes varied, but had a negligible impact on the recorded results.

Droplets extruded in both air and 1 M HCl were allowed at least 2 h to establish an equilibrium tail, although liquid metal droplets extruded into air often did not require as long of a time as those in HCl. Droplets extruded into 0.1 M NaOH were allowed to come to an equilibrium for at least 40 min, and upward of 2 h, although this length of time was not necessary as the droplet had established its equilibrium surface tension before the analysis even began. Liquid metal droplet extruded into water were allowed at least 10 h to come to an equilibrium, though many were able to establish an equilibrium before this time, the additional hours enabled a proper determination of equilibrium status.

XPS and Sample Preparation: XPS measurements were performed using a Kratos Axis Ultra DLD spectrometer with monochromatic Al Kα radiation ($h\nu$ = 1486.6 eV). The high-resolution Ga 2p3/2, O 1s, Sn 3d, In 3d, C 1s, Cl 2p, and Ga 3d/Sn 4d/In 4d spectra were collected at constant pass energy (PE) with a PE of 20 eV. A built-in commercial Kratos charge neutralizer was used to achieve better resolution. Binding energy (BE) values refer to the Fermi edge and the energy scale was calibrated using Au 4f7/2 at 84.0 eV and Cu 2p3/2 at 932.67 eV. The photoemission peak positions were charge corrected to the adventitious carbon signal of C 1s at 284.8 eV. Spectra were analyzed using the CasaXPS software program, version 2.3.16 PR 1.6 (Casa Software Ltd.). A Shirley background was subtracted from each region before curve fitting; metal components were fitted with asymmetric Gaussian–Lorentzian peaks with tail dampening (CasaXPS Lineshapes ≈ LF(1,1.4,20,50)) and oxide components—with Gaussian–Lorentzian peaks (CasaXPS Lineshapes ≈ SGL(10)). Since the Ga 3d/Sn 4d/In 4d region contains the contribution of all three metal of interest, we focused qualitative/quantitative analysis on this region. Spin–orbit coupling doublets of the

Sn 4d (4d5/2 and 4d3/2), Ga 3d (3d5/2 and 3d3/2), and In 4d (4d5/2 and 4d3/2) electron levels were subject to spacing constraints of 1.10, 0.45, and 0.85 eV, respectively. The intensity ratio of the spin–orbit coupling doublets for the d levels (d5/2 and d3/2) was fixed to be 3:2. The atomic concentrations of the chemical elements on the near-surface region were estimated after the subtraction of a Shirley-type background, taking into account the corresponding Scofield atomic sensitivity factors and inelastic mean free path (IMFP) of photoelectrons using standard procedures in the CasaXPS software.

The following protocol was used to prepare samples for the XPS measurements. (a) Glass substrates were exposed to oxygen plasma to encourage the galinstan droplets to adhere to the surface. (b) Droplets of galinstan were immediately placed on the substrates, and were allowed to sit for 2 d to maximize adhesion between the droplet and the substrate (so the droplets do not move during treatment and testing). (c) Samples were then briefly rinsed in a chemical etchant bath of NaOH (1 M) or HCl (1 M) to alter the droplet's surface chemistry for 20 and 45 s, respectively. This is longer than is needed to create a visible change of the droplets' surface chemistry, but the extra time was to ensure that all oxide had been removed. (d) The two samples that were rinsed in water were quickly dried first by wicking away the majority of the remaining water (via absorption), with the remaining water forcibly evaporated by passing dry nitrogen across the substrate and droplet. As-prepared samples were loaded to the XPS spectrometer through a load-lock.

Supporting Information

Supporting Information is available from the Wiley Online Library or from the author.

Acknowledgements

The authors would like to thank Prof. Kendra Erk (Materials Science Engineering, Purdue University) for her assistance with the surface tension goniometry. This project was funded by a NASA Early Career Faculty award (Grant No. NNX14AO52G). Any opinion, findings, and conclusions or recommendations expressed in this material are those of the authors and do not necessarily reflect the views of the National Aeronautics and Space Administration.

Received: September 22, 2016
Revised: October 26, 2016
Published online: January 5, 2017

[1] R. J. Whitney, *J. Physiol.* **1953**, *121*, 1.
[2] R. K. Kramer, *Micro- and Nanotechnology Sensors, Systems, and Applications VII*, Vol. *9467*, **2015**, pp. 946707–946709.
[3] J. C. Case, E. L. White, R. K. Kramer, *Smart Mater. Struct.* **2016**, *25*, 045018.
[4] N. Farrow, N. Correll, in *2015 IEEE/RSJ International Conf. Intelligent Robots and Systems (IROS)*, **2015**, pp. 2317–2323.
[5] R. A. Bilodeau, E. L. White, R. K. Kramer, in *2015 IEEE/RSJ Int. Conf. Intelligent Robots and Systems (IROS)*, **2015**, pp. 2324–2329.
[6] J. Tersoff, D. E. Jesson, W. X. Tang, *Science* **2009**, *324*, 236.
[7] W. X. Tang, C. X. Zheng, Z. Y. Zhou, D. E. Jesson, J. Tersoff, *IBM J. Res. Dev.* **2011**, *55*, 10:1.
[8] J. Wu, Z. M. Wang, A. Z. Li, M. Benamara, S. Li, G. J. Salamo, *PLoS ONE* **2011**, *6*, e20765.
[9] S. Kanjanachuchai, C. Euaruksakul, *ACS Appl. Mater. Interfaces* **2013**, *5*, 7709.
[10] E. Hilner, A. A. Zakharov, K. Schulte, P. Kratzer, J. N. Andersen, E. Lundgren, A. Mikkelsen, *Nano Lett.* **2009**, *9*, 2710.
[11] M. D. Dickey, *ACS Appl. Mater. Interfaces* **2014**, *6*, 18369.
[12] E. Palleau, S. Reece, S. C. Desai, M. E. Smith, M. D. Dickey, *Adv. Mater.* **2013**, *25*, 1589.
[13] M. R. Khan, G. J. Hayes, J.-H. So, G. Lazzi, M. D. Dickey, *Appl. Phys. Lett.* **2011**, *99*, 013501.
[14] Y.-L. Park, C. Majidi, R. Kramer, P. Bérard, R. J. Wood, *J. Micromech. Microeng.* **2010**, *20*, 125029.
[15] V. Sivan, S.-Y. Tang, A. P. O'Mullane, P. Petersen, N. Eshtiaghi, K. Kalantar-zadeh, A. Mitchell, *Adv. Funct. Mater.* **2013**, *23*, 144.
[16] W. Zhang, J. Z. Ou, S.-Y. Tang, V. Sivan, D. D. Yao, K. Latham, K. Khoshmanesh, A. Mitchell, A. P. O'Mullane, K. Kalantar-zadeh, *Adv. Funct. Mater.* **2014**, *24*, 3799.
[17] X. Tang, S.-Y. Tang, V. Sivan, W. Zhang, A. Mitchell, K. Kalantar-zadeh, K. Khoshmanesh, *Appl. Phys. Lett.* **2013**, *103*, 174104.
[18] V. Kocourek, Ch. Karcher, M. Conrath, D. Schulze, *Phys. Rev. E* **2006**, *74*, 026303.
[19] J. Zhang, Y. Yao, L. Sheng, J. Liu, *Adv. Mater.* **2015**, *27*, 2648.
[20] J. Zhang, R. Guo, J. Liu, *J. Mater. Chem. B* **2016**, *4*, 5349.
[21] S.-Y. Tang, V. Sivan, K. Khoshmanesh, A. P. O'Mullane, X. Tang, B. Gol, N. Eshtiaghi, F. Lieder, P. Petersen, A. Mitchell, K. Kalantar-zadeh, *Nanoscale* **2013**, *5*, 5949.
[22] M. R. Khan, C. B. Eaker, E. F. Bowden, M. D. Dickey, *Proc. Natl. Acad. Sci. USA* **2014**, *111*, 14047.
[23] L. Sheng, J. Zhang, J. Liu, *Adv. Mater.* **2014**, *26*, 6036.
[24] S.-Y. Tang, K. Khoshmanesh, V. Sivan, P. Petersen, A. P. O'Mullane, D. Abbott, A. Mitchell, K. Kalantar-zadeh, *Proc. Natl. Acad. Sci. USA* **2014**, *111*, 3304.
[25] J. Y. Zhu, S.-Y. Tang, K. Khoshmanesh, K. Ghorbani, *ACS Appl. Mater. Interfaces* **2016**, *8*, 2173.
[26] M. Mohammed, R. Sundaresan, M. D. Dickey, *ACS Appl. Mater. Interfaces* **2015**, *7*, 23163.
[27] Y. Y. Yao, J. Liu, *RSC Adv.* **2016**, *6*, 56482.
[28] M. D. Dickey, R. C. Chiechi, R. J. Larsen, E. A. Weiss, D. A. Weitz, G. M. Whitesides, *Adv. Funct. Mater.* **2008**, *18*, 1097.
[29] T. Liu, P. Sen, C. J. Kim, *J. Microelectromech. Syst.* **2012**, *21*, 443.
[30] Q. Xu, N. Oudalov, Q. Guo, H. M. Jaeger, E. Brown, *Phys. Fluids* **2012**, *24*, 063101.
[31] K. Doudrick, S. Liu, E. M. Mutunga, K. L. Klein, V. Damle, K. K. Varanasi, K. Rykaczewski, *Langmuir* **2014**, *30*, 6867.
[32] Q. Xu, E. Brown, H. M. Jaeger, *Phys. Rev. E* **2013**, *87*, 043012.
[33] I. D. Joshipura, H. R. Ayers, C. Majidi, M. D. Dickey, *J. Mater. Chem. C* **2015**, *3*, 3834.
[34] W. Irshad, D. Peroulis, in *Proc. 9th Int. Workshop on Micro and Nanotechnology for Power Generation and Energy Conversion Applications (PowerMEMS)*, **2009**, pp. 127–129.
[35] G. Li, M. Parmar, D. Kim, J.-B. Lee, D.-W. Lee, *Lab Chip* **2013**, *14*, 200.
[36] D. Kim, P. Thissen, G. Viner, D.-W. Lee, W. Choi, Y. J. Chabal, J.-B. Lee, *ACS Appl. Mater. Interfaces* **2013**, *5*, 179.
[37] D. Kim, Y. Lee, D.-W. Lee, W. Choi, K. Yoo, J.-B. Lee, *Sens. Actuators, B* **2015**, *207*, 199.
[38] G. Li, X. Wu, D.-W. Lee, *Lab Chip* **2016**, *16*, 1366.
[39] N. Ilyas, D. P. Butcher, M. F. Durstock, C. E. Tabor, *Adv. Mater. Interfaces* **2016**, *3*, 1500665.
[40] J. C. Case, E. L. White, R. K. Kramer, *Soft Rob.* **2015**, *2*, 80.
[41] The bond number is the non-dimensional parameter used to characterize the influence of surface forces (surface tension) versus body forces (gravity) on a droplet. Bond numbers closer to zero indicate spherical droplets, with surface tension dominating over the influence of gravitational forces.
[42] M. Hoorfar, A. W. Neumann, *Adv. Colloid Interface Sci.* **2006**, *121*, 25.
[43] J. D. Berry, M. J. Neeson, R. R. Dagastine, D. Y. C. Chan, R. F. Tabor, *J. Colloid Interface Sci.* **2015**, *454*, 226.

[44] M. R. Khan, C. Trlica, J.-H. So, M. Valeri, M. D. Dickey, *ACS Appl. Mater. Interfaces* **2014**, *6*, 22467.
[45] H. P. Wampler, D. Y. Zemlyanov, K. Lee, D. B. Janes, A. Ivanisevic, *Langmuir* **2008**, *24*, 3164.
[46] M. S. Makowski, D. Y. Zemlyanov, J. A. Lindsey, J. C. Bernhard, E. M. Hagen, B. K. Chan, A. A. Petersohn, M. R. Medow, L. E. Wendel, D. Chen, J. M. Canter, A. Ivanisevic, *Surf. Sci.* **2011**, *605*, 1466.
[47] R. Paul, R. G. Reifenberger, T. S. Fisher, D. Y. Zemlyanov, *Chem. Mater.* **2015**, *27*, 5915.
[48] A. Gharachorlou, M. D. Detwiler, X.-K. Gu, L. Mayr, B. Klotzer, J. Greeley, R. G. Reifenberger, W. N. Delgass, F. H. Ribeiro, D. Y. Zemlyanov, *ACS Appl. Mater. Interfaces* **2015**, *7*, 16428.
[49] J. Čechal, T. Matlocha, J. Polčák, M. Kolíbal, O. Tomanec, R. Kalousek, P. Dub, T. Šikola, *Thin Solid Films* **2009**, *517*, 1928.
[50] C. V. Ramana, E. J. Rubio, C. D. Barraza, A. M. Gallardo, S. McPeak, S. Kotru, J. T. Grant, *J. Appl. Phys.* **2014**, *115*, 043508.

